In Vivo Imaging of Macrophage Activity in the Coronary Arteries Using ^{68}Ga-DOTATATE PET/CT: Correlation with Coronary Calcium Burden and Risk Factors

Axel Rominger[1], Tobias Saam[2], Eva Vogl[1], Christopher Übleis[1], Christian la Fougère[1], Stefan Förster[1], Alexander Haug[1], Paul Cumming[1], Maximilian F. Reiser[2], Konstantin Nikolaou[2], Peter Bartenstein[1], and Marcus Hacker[1]

[1]Department of Nuclear Medicine, University of Munich, Munich, Germany; and [2]Institute of Clinical Radiology, University of Munich, Munich, Germany

We measured the uptake of the somatostatin receptor ligand ^{68}Ga-[1,4,7,10-tetraazacyclododecane-*N,N′,N″,N‴*-tetraacetic acid]-D-Phe[1],Tyr[3]-octreotate (DOTATATE) in the left anterior descending coronary artery (LAD) in association with calcified plaques (CPs) and cardiovascular risk factors. **Methods:** Seventy consecutive tumor patients were examined by whole-body ^{68}Ga-DOTATATE contrast-enhanced PET/CT. Blood-pool–corrected standardized uptake value (target-to-background ratio) was measured in the LAD, and CT images were used to detect CP. Cardiovascular risk factors and history of prior cardiovascular events were recorded. **Results:** ^{68}Ga-DOTATATE uptake was detectable in the LAD of all patients. Target-to-background ratio in the LAD correlated significantly with the presence of CP ($R = 0.34$; $P < 0.01$), prior vascular events ($R = 0.26$; $P < 0.05$), and male sex ($R = 0.29$; $P < 0.05$), whereas CP correlated with these parameters but also with age ($R = 0.34$; $P < 0.01$) and hypertension ($R = 0.25$; $P < 0.05$). **Conclusion:** In a series of oncologic patients, those with prior cardiovascular events and calcified atherosclerotic plaques showed significantly increased ^{68}Ga-DOTATATE uptake in the LAD, suggesting a potential role of this tracer for plaque imaging in the coronary arteries.

Key Words: atherosclerosis; plaque imaging; ^{68}Ga-DOTATATE PET/CT; cardiovascular; coronary arteries

Atherosclerosis is one of the leading causes of morbidity and mortality in the world (*1*), accounting for most myocardial infarctions and sudden cardiac deaths (*2*). New imaging methods can help identify high-risk patients who bear vascular lesions that are vulnerable to thrombosis, the so-called vulnerable plaques. Active inflammation is implicated in initiation, progression, and disruption of vulnerable plaques and consequently represents an emerging target for the imaging and treatment of atherosclerosis. Local inflammatory processes can now be assessed by noninvasive imaging methods intended to identify the vulnerable plaque on the basis of its physiologic properties (*3,4*).

Whole-body ^{18}F-FDG PET/CT is a reliable and well-established method to image and quantify plaque inflammation (*5*). There was good correlation between carotid plaque ^{18}F-FDG uptake in vivo and macrophage staining from the corresponding histologic sections (*6*). Furthermore, there was a weak but highly significant correlation between ^{18}F-FDG uptake and cardiovascular risk factors (*7*) and the occurrence of future cardiovascular events (*8*). However, most of this work has been performed on relatively large arteries, such as the aorta or the carotid arteries. Although pathologic features in these arteries are likely representative of a general atherosclerotic disease, it is the thromboembolic complications arising in the coronary arteries that are responsible for most deaths (*9*). Furthermore, most of these fatal cardiovascular events occur in coronary arteries with less than 50% stenosis (*10*), indicating that information about luminal stenosis is insufficient to predict the vulnerability of a plaque. Although ^{18}F-FDG can serve as a metabolic marker for inflamed plaques in the coronary arteries, its applicability is limited by poor control of physiologic uptake of ^{18}F-FDG in the myocardium, which frequently obscures the vascular pathology (*11*).

As an alternative to the visualization of macrophages with ^{18}F-FDG PET, somatostatin receptors of subtype 2 (SSTR$_2$), which are expressed by macrophages (*12*), can be detected with the PET ligand ^{68}Ga-[1,4,7,10-tetraazacyclododecane-*N,N′,N″,N‴*-tetraacetic acid]-D-Phe[1],Tyr[3]-octreotate (DOTATATE) (*13*). Unlike the case of ^{18}F-FDG, there

is no physiologic ^{68}Ga-DOTATATE uptake in the myocardium, which permits more clear and consistent detection of macrophage accumulation in the coronary arteries.

The purpose of the present study was to correlate ^{68}Ga-DOTATATE uptake in the left anterior descending coronary artery (LAD) with the presence of calcified plaques (CPs) and cardiovascular risk factors. To this end, we retrospectively reanalyzed ^{68}Ga-DOTATATE scans that had been obtained for the investigation of neuroendocrine tumors.

MATERIAL AND METHODS

Patients

The study group consisted of 70 consecutive patients who had been referred to our institution for a contrast-enhanced PET/CT scan because of the presence of a neuroendocrine tumor. The study protocol was approved by the local clinical institutional review board and complied with the Declaration of Helsinki. None of the patients was under current steroid medication or other treatments known to affect vessel wall metabolism. Age, body mass index (BMI), and common cardiovascular risk factors such as hypertension, hypercholesterolemia, smoking habits, family history, prior vascular events defined as myocardial infarction, revascularization procedures or stroke, and diabetes mellitus were documented from charts.

Imaging Technique

All patients underwent ^{68}Ga-DOTATATE PET/CT on a Gemini scanner (Philips), consisting of a germanium oxyorthosilicate full-ring PET scanner and a 2-detector-row CT scanner. Patients received 20 mg of furosemide at the same time as an intravenous injection of 3 MBq of ^{68}Ga-DOTATATE (mean dose, 211 MBq) per kilogram. Sixty minutes after radiotracer administration, transmission data were acquired using a whole-body low-dose CT scan with conventional parameters. Next, a contrast-enhanced CT scan (Ultravist 370, 370 mg of iodine/mL; Bayer-Schering AG) with a slice thickness of 3 mm (195 mAs, 120 kV, 512×512 matrix, 5 mm/s increment, 0.5-s rotation time, and 1.5 pitch index) was obtained. Finally, caudocephalad PET emission recordings were acquired in 3-dimensional mode with a 144×144 matrix. After scatter and decay correction, PET data were reconstructed iteratively with and without attenuation correction and then reoriented in axial, sagittal, and coronal slices. A fully 3-dimensional reconstruction algorithm based on the row-action maximum-likelihood algorithm was applied with the PET-View software (Philips).

Image Analysis

^{68}Ga-DOTATATE Uptake. PET/CT scans were examined by an experienced reader who was unaware of patient and clinical information. Maximal standardized uptake values (SUVs) were measured from the left sinus of Valsalva to the outlet of the first diagonal branch of the LAD, which we herein define as LAD. We manually placed regions of interest (ROIs) of fixed size in all patients. The size was chosen to match the lumen of the vessel. Finally, the correct placement of the ROI within the lumen of the coronary artery was in each case visually verified by inspection in all 3 planes, using the zoom display tool and moving the ROIs along the long axis to find the regions of maximal SUV (Fig. 1).

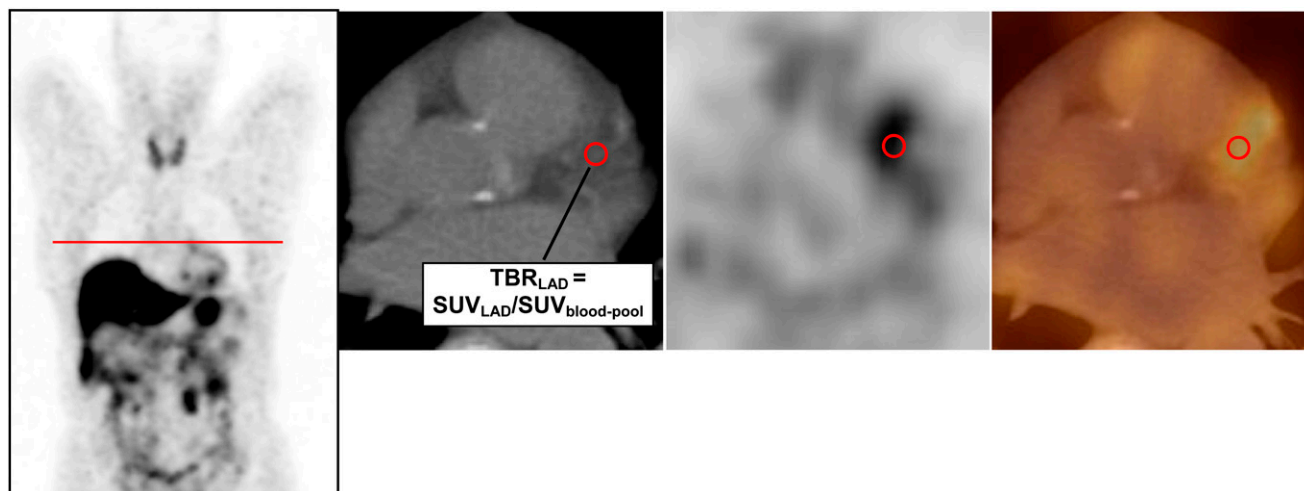Blood-pool SUV was the mean from 3 ROIs placed in the mid lumen of the vena cava inferior and the vena cava

$$TBR_{LAD} = SUV_{LAD}/SUV_{blood-pool}$$

FIGURE 1. PET/CT image analysis. Example of SUV measurement in LAD. PET/CT images of 64-y-old woman with history of smoking (40 pack-years), diabetes, and hypercholesterolemia. From left to right: first panel shows coronal slice of PET scan. Red line indicates same axial slice as that presented in other 3 images. Second panel shows axial CT image of coronary artery, which was used to localize LAD. Red circle in panels 2, 3, and 4 indicates ROI, placed in LAD. Third panel shows axial PET slice, and fourth panel shows fused CT and PET image. SUV was measured on fused PET/CT images along course of vessel. Maximum SUV in this patient was 0.9, and mean venous SUV in upper and lower vena cava was 0.5, resulting in target–to–background ratio (TBR) of 1.8.

superior. The maximal SUV of the LAD was divided by blood-pool SUV, yielding a target-to-background ratio (TBR).

In addition, the major aortic divisions (ascending, arch, descending, abdominal) and the iliac and common carotid arteries were analyzed for the presence of ^{68}Ga-DOTATATE uptake. We placed simple circular ROIs on the coregistered PET/CT slices, as described previously (*8*).

Plaque Burden. The CT scans were examined for the presence of CPs in the wall of the LAD (vascular attenuation > 130 Hounsfield units) (*14*). Patients were divided into those with CP and those without discernible CP. Soft plaques were not discernible in the LAD. The major peripheral arteries listed above were also scanned for presence of calcifications.

Reproducibility. To assess intra- and interreader reproducibility, TBR and CP measurements were repeated 8 wk after the initial review by the same reviewer and by a second reviewer, for the calculation of intraclass correlation coefficients (ICCs) with 95% confidence intervals (CIs).

Statistical Analysis

Categoric variables are presented with absolute and relative frequencies, whereas continuous variables are presented as mean and SD. For between-group comparisons for the TBR, unpaired Student *t* tests were used for parametric data, and Mann–Whitney *U* rank sum tests were used for nonparametric data. The Pearson correlation coefficient was used to correlate TBR with CP and with age, BMI, and the occurrence of cardiovascular risk factors. To identify the optimal TBR threshold value, receiver-operating-characteristic analysis was performed (*15*).

RESULTS

Patient Population

^{68}Ga-DOTATATE uptake measurements in the LAD were feasible in all patients. Relevant patients' baseline characteristics are reported in Table 1.

Correlation of Baseline Parameters

Table 2 shows the correlations of baseline characteristics with TBR and CP in the LAD. Within the 70 patients, significant correlations were observed between TBR and male sex ($R = 0.29$; $P < 0.05$) and prior vascular events ($R = 0.26$; $P < 0.05$). Furthermore, there was a significant correlation between the presence of TBR and CP ($R = 0.34$; $P < 0.01$; Fig. 2). In 14 of 25 (56%) cases, the uptake was not colocalized in the CP.

CP correlated significantly with age ($R = 0.34$; $P < 0.01$), male sex ($R = 0.39$; $P < 0.01$), hypertension ($R = 0.25$; $P < 0.05$), and prior vascular events ($R = 0.37$; $P < 0.01$).

Images from patients with high TBR are clearly distinct from low-TBR images (Fig. 3). Receiver-operating-characteristic analysis indicated that a cutoff TBR greater than or equal to 1.5 gave an optimal threshold for specifically distinguishing between patients with and without coronary calcifications. Of the 12 high-uptake patients, 75% also had

TABLE 1. Baseline Characteristics of Study Population (*n* = 70)

Parameter	Value
Age (y)	
Mean ± SD	58.9 ± 11.7
Range	30–81
Men (*n*)	38 (54.3%)
BMI	
Mean ± SD	25.1 ± 3.7
Range	19.0–49.0
Cardiovascular risk factors (*n*)	
Hypercholesterolemia	20 (28.6%)
Hypertension	36 (51.4%)
Active smoker	8 (11.4%)
Diabetes mellitus	9 (12.9%)
Family history of cardiovascular disease	10 (14.3%)
Prior vascular event	14 (20.0%)
Coronary CPs present	25 (35.7%)
TBR in LAD	
Mean ± SD	1.21 ± 0.30
Range	0.63–2.00
Therapy (*n*)	
Statin	11 (15.7%)
Sandostatin	9 (12.9%)

CPs within the LAD, versus only 28% of the low-uptake patients.

There was a significant correlation between TBR and presence of CP in the abdominal aorta ($R = 0.256$; $P < 0.05$), the right iliac artery ($R = 0.273$; $P < 0.05$), and both common carotid arteries (right, $R = 0.358$; $P < 0.01$; left, $R = 0.297$; $P < 0.05$). Furthermore, there were significant correlations ($P < 0.05$) between TBR and male sex and also prior cardio- or cerebrovascular events in the common carotid arteries.

Patients undergoing statin or Sandostatin (Novartis Pharma AG) therapy, compared with the other patients, did not show significantly altered ^{68}Ga-DOTATATE uptake.

TABLE 2. Correlation of Baseline Characteristics with TBR in LAD and CP in LAD

Parameter	TBR in LAD	CP in LAD
Age	NS	0.34*
Male sex	0.29†	0.39*
BMI	NS	NS
Hypertension	NS	0.25†
Smoking	NS	NS
Family history	NS	NS
Diabetes	NS	NS
Hypercholesterolemia	NS	NS
Prior vascular event	0.26†	0.37*
TBR in LAD	1.00	0.34*
CP in LAD		1.00

*$P < 0.01$.
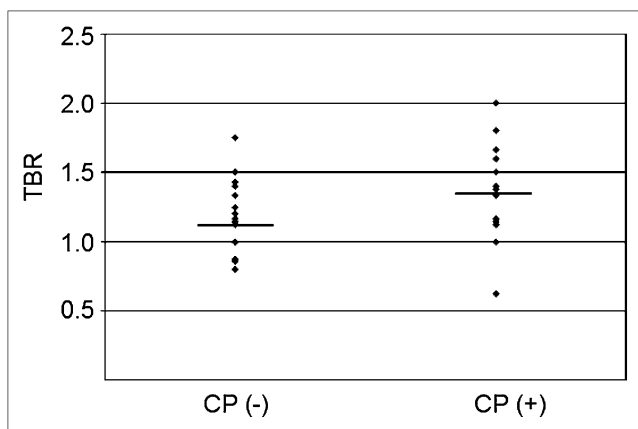†$P < 0.05$.
NS = statistically not significant.

FIGURE 2. Relation of TBR to calcification. Scatter plot shows individual ratios for all patients, separated into those with CP (CP (+)) and those without CP (CP (−)). Mean values are indicated with horizontal line.

Reproducibility

The intrareader ICC for TBR measurements was 0.97 (95% CI, 0.93–0.99), and the interreader ICC was 0.94 (95% CI, 0.89–0.97).

DISCUSSION

We present the first quantitation of ^{68}Ga-DOTATATE uptake in the anterior descending coronary artery using PET/CT. We found a significant correlation between ^{68}Ga-DOTATATE uptake and the presence of vessel wall calcifications. On stratifying the subjects into groups with high and low tracer uptake, we found that most of the patients with high tracer uptake also had calcifications (seen in only a third of the patients with low ^{68}Ga-DOTATATE uptake) in the LAD. Our finding of 44% colocalization is in line with previous studies conducted with ^{18}F-FDG, reviewed by Kato et al. (16). Furthermore, patients with prior cardiovascular events had significantly increased ^{68}Ga-DOTATATE uptake in the LAD, suggesting this radiotracer as a potential biomarker for the identifica-

tion of vulnerable coronary artery plaques and indeed in other major vessels, as already shown for ^{18}F-FDG.

Molecular Background

Several publications have demonstrated the expression of somatostatin subtype 1 receptors and $SSTR_2$ on human macrophages (12,17). ^{68}Ga-DOTATATE, which has hitherto been used for the assessment of neuroendocrine tumors, has a high affinity and selectivity for $SSTR_2$ and is rapidly cleared from nontarget tissues, thus offering good target-to-nontarget imaging properties (13). Indeed, the myocardium was devoid of significant ^{68}Ga-DOTATATE uptake, which is an important precondition for using this tracer for the assessment of atherosclerosis in the coronary arteries.

Comparison to Other Biomarkers of Atherosclerosis

Several previous studies reported significant correlations between the presence of cardiovascular risk factors and ^{18}F-FDG uptake in large arteries (7,18,19). Moreover, increased ^{18}F-FDG uptake in large arteries was recently demonstrated in oncologic patients with prior cardiovascular events (19) and in oncologic patients who had a cerebro- or cardiovascular event during follow-up (8). This increased ^{18}F-FDG uptake is presumably an indicator of elevated metabolic activity in macrophages resident in the inflamed plaques. Macrophage proliferation has been documented in culprit lesions after plaque ruptures, leading to myocardial infarction or sudden cardiac death (9). In the only previous ^{18}F-FDG PET study of the coronary arteries, a series of 32 patients was investigated according to oncologic indications (11); of the 17 patients in whom arterial wall ^{18}F-FDG uptake was discernible, 15 proved to have stenoses of more than 50% on coronary angiography. Nonetheless, general application of the approach is hampered by the occurrence of significant ^{18}F-FDG uptake in the myocardium of nearly one half of the patients, despite prescan fasting or the use of a low-carbohydrate, high-fat diet. Thus, the low myocardial uptake of ^{68}Ga-DOTATATE presents an advantage over ^{18}F-FDG for the detection of macrophage infiltration of coronary vessels; we could evaluate ^{68}Ga-DOTATATE
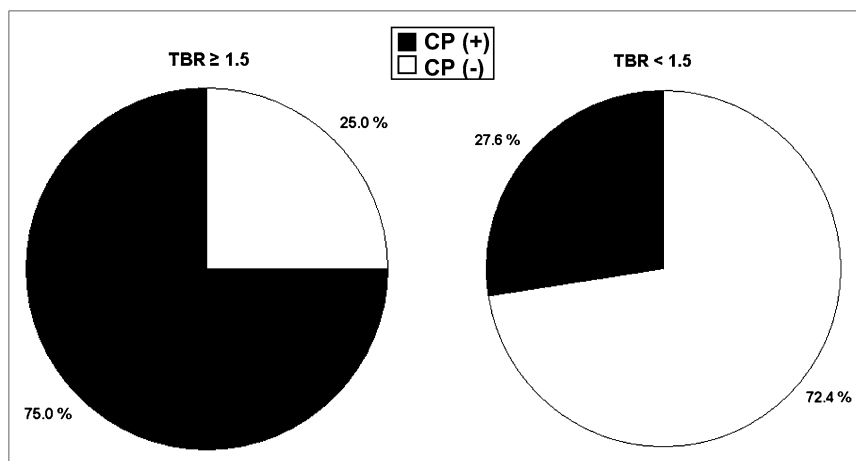

FIGURE 3. Proportion of ^{68}Ga-DOTATATE uptake and calcifications in LAD. Patients with high DOTATATE uptake (TBR ≥ 1.5) also show high percentage of CPs within LAD (left diagram), whereas patients with low DOTATATE uptake (TBR < 1.5) had low percentage of CPs within LAD (right diagram).

uptake in the LAD in all 70 of our patients, with excellent intra- and interreader reproducibility for the TBR values, comparable to those obtained earlier for ^{18}F-FDG uptake measurements in peripheral vessels (*20*).

Future PET/CT studies using dedicated CT and electro-cardiogram-gated PET should enable the measurement of ^{68}Ga-DOTATATE uptake in the whole coronary artery tree while also obtaining CT calcium scores. In the present cross-sectional study, the magnitude of CP in the LAD of oncology patients correlated with most cardiovascular risk factors, underlining the inherent association of CPs with the presence of atherosclerosis (*21*). Macrophages have been targeted as a marker of plaque vulnerability in imaging studies with several radiopharmaceuticals other than ^{18}F-FDG. Kietselaer et al. investigated 4 preoperative carotid endarterectomy patients with ^{99m}Tc-annexin A5, a labeled plasma protein that binds to cell membranes of apoptotic macrophages (*22*); increased radiotracer uptake was observed in patients with a recent prior cardiovascular event who also showed histopathologic features of unstable plaque. Other studies have used choline derivatives, which are transported into activated macrophages and incorporated into the cell membrane; elevated uptake of these tracers is reported in the walls of vessels with and without calcifications (*16*).

Limitations

Because this study was performed in tumor patients, the findings may be imperfectly generalizable to investigations of vascular disease per se. Although the stringent national guidelines for recruitment of healthy control subjects (related to the radiation exposure) necessitated the use of an ill cohort, the present findings make a compelling rationale for conducting prospective PET/CT vascular examinations using ^{68}Ga-DOTATATE in noncancer patients. Furthermore, in these patients noncardiac CT scans were obtained so that the proximal portion of the left coronary artery only could be reliably evaluated.

CONCLUSION

On the basis of in vitro findings of the expression of $SSTR_2$ on macrophages, we measured ^{68}Ga-DOTATATE uptake in the LAD of a series of oncologic patients. Those patients with prior cardiovascular events and calcified atherosclerotic plaques showed significantly increased ^{68}Ga-DOTATATE uptake in the LAD, suggesting a potential role of this tracer for plaque imaging and characterization in the coronary arteries.

ACKNOWLEDGMENT

REFERENCES

1. Lloyd-Jones D, Adams R, Carnethon M, et al. Heart disease and stroke statistics: 2009 update—a report from the American Heart Association Statistics Committee and Stroke Statistics Subcommittee. *Circulation.* 2009;119:e21–e181.
2. Naghavi M, Libby P, Falk E, et al. From vulnerable plaque to vulnerable patient: a call for new definitions and risk assessment strategies: part I. *Circulation.* 2003;108:1664–1672.
3. Saam T, Hatsukami TS, Takaya N, et al. The vulnerable, or high-risk, atherosclerotic plaque: noninvasive MR imaging for characterization and assessment. *Radiology.* 2007;244:64–77.
4. Langer HF, Haubner R, Pichler BJ, Gawaz M. Radionuclide imaging: a molecular key to the atherosclerotic plaque. *J Am Coll Cardiol.* 2008;52:1–12.
5. Rudd JH, Myers KS, Bansilal S, et al. [18]Fluorodeoxyglucose positron emission tomography imaging of atherosclerotic plaque inflammation is highly reproducible: implications for atherosclerosis therapy trials. *J Am Coll Cardiol.* 2007;50:892–896.
6. Tawakol A, Migrino RQ, Bashian GG, et al. In vivo ^{18}F-fluorodeoxyglucose positron emission tomography imaging provides a noninvasive measure of carotid plaque inflammation in patients. *J Am Coll Cardiol.* 2006;48:1818–1824.
7. Yun M, Jang S, Cucchiara A, Newberg AB, Alavi A. [18]F FDG uptake in the large arteries: a correlation study with the atherogenic risk factors. *Semin Nucl Med.* 2002;32:70–76.
8. Rominger A, Saam T, Wolpers S, et al. ^{18}F-FDG PET/CT identifies patients at risk for future vascular events in an otherwise asymptomatic cohort with neoplastic disease. *J Nucl Med.* 2009;50:1611–1620.
9. Finn AV, Nakazawa G, Narula J, Virmani R. Culprit plaque in myocardial infarction going beyond angiography. *J Am Coll Cardiol.* 2007;50:2204–2206.
10. Ambrose JA, Tannenbaum MA, Alexopoulos D, et al. Angiographic progression of coronary artery disease and the development of myocardial infarction. *J Am Coll Cardiol.* 1988;12:56–62.
11. Wykrzykowska J, Lehman S, Williams G, et al. Imaging of inflamed and vulnerable plaque in coronary arteries with ^{18}F-FDG PET/CT in patients with suppression of myocardial uptake using a low-carbohydrate, high-fat preparation. *J Nucl Med.* 2009;50:563–568.
12. Armani C, Catalani E, Balbarini A, Bagnoli P, Cervia D. Expression, pharmacology, and functional role of somatostatin receptor subtypes 1 and 2 in human macrophages. *J Leukoc Biol.* 2007;81:845–855.
13. Breeman WA, de Jong M, de Blois E, Bernard BF, Konijnenberg M, Krenning EP. Radiolabelling DOTA-peptides with [68]Ga. *Eur J Nucl Med Mol Imaging.* 2005;32:478–485.
14. Agatston AS, Janowitz WR, Hildner FJ, Zusmer NR, Viamonte M Jr, Detrano R. Quantification of coronary artery calcium using ultrafast computed tomography. *J Am Coll Cardiol.* 1990;15:827–832.
15. Hanley JA, McNeil BJ. A method of comparing the areas under receiver operating characteristic curves derived from the same cases. *Radiology.* 1983; 148:839–843.
16. Kato K, Schober O, Ikeda M, et al. Evaluation and comparison of ^{11}C-choline uptake and calcification in aortic and common carotid arterial walls with combined PET/CT. *Eur J Nucl Med Mol Imaging.* 2009;36:1622–1628.
17. Elliott DE, Li J, Blum AM, Metwali A, Patel YC, Weinstock JV. SSTR2A is the dominant somatostatin receptor subtype expressed by inflammatory cells, is widely expressed and directly regulates T cell IFN-gamma release. *Eur J Immunol.* 1999;29:2454–2463.
18. Ben-Haim S, Kupzov E, Tamir A, Israel O. Evaluation of ^{18}F-FDG uptake and arterial wall calcifications using ^{18}F-FDG PET/CT. *J Nucl Med.* 2004;45:1816–1821.
19. Paulmier B, Duet M, Khayat R, et al. Arterial wall uptake of fluorodeoxyglucose on PET imaging in stable cancer disease patients indicates higher risk for cardiovascular events. *J Nucl Cardiol.* 2008;15:209–217.
20. Rudd JH, Myers KS, Bansilal S, et al. Atherosclerosis inflammation imaging with ^{18}F-FDG PET: carotid, iliac, and femoral uptake reproducibility, quantification methods, and recommendations. *J Nucl Med.* 2008;49:871–878.
21. Budoff MJ, Shaw LJ, Liu ST, et al. Long-term prognosis associated with coronary calcification: observations from a registry of 25,253 patients. *J Am Coll Cardiol.* 2007;49:1860–1870.
22. Kietselaer BL, Reutelingsperger CP, Heidendal GA, et al. Noninvasive detection of plaque instability with use of radiolabeled annexin A5 in patients with carotid-artery atherosclerosis. *N Engl J Med.* 2004;350:1472–1473.